# Dense Network of O–H···O and C–H···O Interactions in the Solid State Structure of n-Pentyl-2-Chloro-2-Deoxy-α-D-manno-Sept 3-Uloside

**ARTICLE** *in* CARBOHYDRATE RESEARCH · JULY 2014

Impact Factor: 1.93 · DOI: 10.1016/j.carres.2014.04.019



**3 AUTHORS**, INCLUDING:

Supriya Dey
Indian Institute of Science
**7** PUBLICATIONS **23** CITATIONS
SEE PROFILE

Krishnayan Basuroy
Indian Institute of Science
**13** PUBLICATIONS **62** CITATIONS
SEE PROFILE

Carbohydrate Research 393 (2014) 37–42

Contents lists available at ScienceDirect

Carbohydrate Research

journal homepage: www.elsevier.com/locate/carres

# Dense network of O—H···O and C—H···O interactions in the solid state structure of *n*-pentyl-2-chloro-2-deoxy-α-D-*manno*-sept 3-uloside

Supriya Dey [a], Krishnayan Basuroy [b], N. Jayaraman [a,*]

[a] Department of Organic Chemistry, Indian Institute of Science, Bangalore 560012, India
[b] Molecular Biophysics Unit, Indian Institute of Science, Bangalore 560012, India

ARTICLE INFO

*Article history:*
Received 26 March 2014
Received in revised form 24 April 2014
Accepted 29 April 2014
Available online 9 May 2014

*Keywords:*
Carbohydrates
Crystallography
Non-covalent interactions
Septanosides
Ulosides

ABSTRACT

Single crystal X-ray structural analysis of a septanoside, namely, *n*-pentyl-2-chloro-2-deoxy sept-3-uloside (**1**) provides many finer details of the molecular structure, in addition to its preferred twist-chair conformation, namely, $^{5,6}TC_{3,4}$ conformation. Structural analysis reveals a dense network of O—H···O, C—H···O and van der Waals interactions that stabilize interdigitized, planar bi-layer structure of the crystal lattice.



## 1. Introduction

Single crystal X-ray structural determination of furanosides and pyranosides provide rich information of covalent and non-covalent forces governing the crystal lattice, conformation, and molecular recognitions.[1] Such studies on seven-membered ring sugars, namely, septanoses and septanosides, gained a scattered interest early. The conformation of septanosides in the solution phase was studied, whereas solid state structure was limited.[2] Sundarlingam and co-workers reported the crystal structure of 1,2:3,4-di-*O*-isopropylidene-5-*O*-chloro-acetyl-α-D-glucoseptanoside in a first instance in 1970.[3] An analysis of torsional angles showed that the septanoside ring adopted a twist-chair conformation, represented as, $^{5,6}C_2$(D).[4] Stevens and co-workers reported solid-state X-ray crystal structures of a number of septanoside derivatives, all closely related in terms of their conformations. As for example, the crystal structures of the epimeric septanoses, namely, 5-*O*-acetyl-1,2:3,4-di-*O*-isopropylidene α-D-galactoseptanose[5] and 5-*O*-acetyl-1,2:3,4-di-*O*-isopropylidene α-D-glucoseptanose showed that the former adopted a twist-boat conformation, $^{1,2}TB_{3,4}$ whereas the latter exhibited twist-chair conformation,[6] represented as $^{4,5}TC_{6,0}$. The differences in the conformations were thought to result from orientations of the dioxolane rings in the septanosides. In the case of D-galactoseptanoside, 1,2-dioxolane and 3,4-dioxolane rings appeared nearly planar and twisted, respectively, that enforced septanoside to adopt a boat conformation. On the other hand, in the case of D-glucoseptanoside, *cis*-fused dioxolane ring adopted a distorted twist form and *trans*-fused ring an envelope form. Interestingly, isomeric 3-*O*-acetyl-1,2:4,5-di-*O*-isopropylidene-α-D-glucoseptanose adopted a chair conformation.[7] In the case of methyl-2,3,4,5-tetra-*O*-acetyl-α-D-glucoseptanoside, single crystal X-ray structural analysis showed a twist-chair conformation ($^{4,5}TC_{6,0}$), in which the axis of symmetry passed through C2,[8] whereas the corresponding β-anomer resided in a chair conformation.[9] Stevens and co-workers also reported the crystal structure of 1,2:3,4-di-*O*-isopropylidene-4-*C*-methylthiomethoxy-β-L-*arabino*-hexoseptanose-5-uloside,[10] in which the septanose ring adopted a boat conformation, $^{3,4,O}B$(L). Recently, synthesis and crystal structure of β-D-glucoseptanoside pentacetate was also reported, though its conformation was not discussed.[11]

Peczuh and co-workers reported the synthesis and crystal structure of D-xylose based oxepine. The crystal structure of 1,6-anhydro-3,4,5-tri-*O*-benzyl-2-deoxy-D-xylo sept-1-enitol showed a twist-chair conformation.[12] Chapleur and co-workers reported the synthesis of septanoses from hexopyranosides and crystal structure of one intermediate, namely, septanosyl chloride.[13] Although synthetic methodologies leading to septanosides and their derivatives are known in great detail, solid-state structures of such septanosides are rather limited. Further, an analysis of

* Corresponding author. Tel.: +91 80 2293 2578; fax: +91 80 2360 0529.
*E-mail address:* jayaraman@orgchem.iisc.ernet.in (N. Jayaraman).

http://dx.doi.org/10.1016/j.carres.2014.04.019
0008-6215/

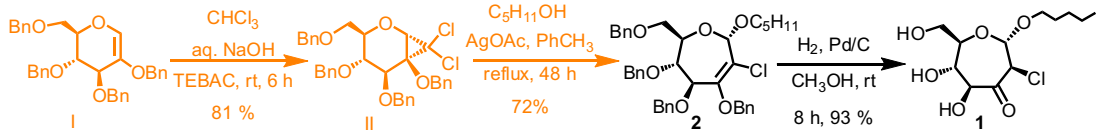


**Scheme 1.**

the non-covalent interactions governing the solid-state structures is rarely described. In our continuing interest to study septanosides and their derivatives, we encounter a septanoside as an important intermediate, which permits to synthesize a range of septanoside derivatives.[14,15] In the course of studies, such an important septanoside intermediate crystallized, which provided an avenue to determine the septanoside conformation and the non-covalent interactions that govern the solid-state structure. Details of the study are reported herein.

## 2. Results and discussion

Synthesis of chloro-oxepine **2**, prepared from oxyglycal precursor **I** and the cyclopropanated derivative **II**, was reported previously.[15] A solution of chloro-oxepine **2** in MeOH (10 mL), in the presence of 10% Pd/C under a positive pressure of $H_2$(g), furnished the desired sept-3-uloside **1**, in an excellent yield (Scheme 1). The structure of **1** was confirmed by $^1$H, $^{13}$C, COSY, and HSQC NMR spectral analyses. The $^3J_{H1\text{-}H2}$ was found to be 7.4 Hz, indicating a *trans*-relationship between H1 and H2. The presence of ketone moiety at C3 was confirmed by the signal at 200.6 ppm, whereas anomeric carbon resonated at 103.1 ppm in the $^{13}$C NMR spectrum.

Single crystals suitable for analysis were obtained upon slow evaporation of a solution of **1** in MeOH. Compound **1** crystallized in the monoclinic C2 space group, with $a = 43.22(2)$, $b = 4.812(3)$, $c = 7.035(3)$ Å, and $\beta = 91.51(2)$ and four molecules constituted the unit cell ($Z = 4$), whereas asymmetric unit contained one molecule (Table 1). ORTEP of **1** is given in Figure 1, all significant bond distances, bond angles and torsion angles are listed in Tables 2 and 3.

An analysis of the C—C bond lengths within the septanoside ring shows that the bond lengths are in the range between 1.579 and 1.464 Å. The C2—Cl bond length (1.776 Å) was found to be higher than other bond lengths, whereas *exo*-cyclic C1—O1 bond length was 1.403 Å (Table 2). The bond lengths C6—O6 and O6—C1 were 1.465 and 1.417 Å, respectively. The shortening C1—O1 bond compared to O6—C1 indicated a significant anomeric effect, as in the case of free sugar derivatives. The bond length 1.189 Å of C3—O3 bond was found to be shortest. The bond length of C—H bonds varied from 0.959 to 0.981 Å. An interesting feature of the ring C—C bond distances was that C1—C2 (1.584 Å) and C3—C4 (1.533 Å) were significantly higher than the remaining *endo*-cyclic C—C bond in **1**. A similar observation was reported previously by Stevens and co-workers.[5]

The bond angles within the septanoside ring were greater than an ideal tetrahedron. The C2—C3—C4 angle (114.7°) showed a slight strain imposed by the trigonal planar carbonyl moiety (Table 3). The large deviation of the bond angle C3—C4—C5 of 121.5° appeared to result from eclipsing interaction between C—OH and C=O, when viewed along C3—C4. The valance bond angles of 115.5° and 112.7° in the sequence C6—O6—C1—O1, respectively, and the torsion angle of −65.0° (C6—O6—C1—O1) indicated the α-configuration at the anomeric center. The *n*-pentyl group oriented antiperiplanar to C2. The torsion angles of C8—O1—C1—O6 of −73.2° and C8—O1—C1—C2 of 166.3° showed that the anomeric substituent has *gauche–trans* orientation with respect to the septanoside ring. On the other hand, the torsion angles of O6—C6—C7—O7 of 64.8° and C5—C6—C7—O7 of −53.3° indicated a *gauche–gauche* orientation of primary hydroxyl group, with respect to the ring oxygen, as well as, to the C5 substituent. The torsion angle of the *n*-pentyl moiety O1—C8—C9—C10 was

**Table 1**
Crystal data and structure refinement parameters

| | |
|---|---|
| *Crystal data* | |
| Chemical formula | $C_{12}H_{21}ClO_6$ |
| Chemical formula weight ($M_r$) | 296.74 |
| Crystal habit, color | Rectangular block |
| Crystal size (mm) | 0.28 × 0.09 × 0.06 |
| Crystallizing solvent | $CH_3OH$ |
| Space group | *C*2 |
| *a* (Å) | 43.22(2) |
| *b* (Å) | 4.812(3) |
| *c* (Å) | 7.035(3) |
| *β* (°) | 91.51(2) |
| Volume (Å$^3$) | 1462.3(12) |
| *Z* | 4 |
| Molecules/asymmetric unit | 1 |
| Calculated density (g/cm$^3$) | 1.339 |
| *Data collection* | |
| Diffractometer | Bruker Axs Kappa ApexII CCD with Mo source |
| Radiation | MoK$_\alpha$ (0.71073 Å) |
| Temperature (K) | 296 (2) |
| Scan mode | ϕ and ω |
| 2$\theta$ max. (°) | 60.08 |
| 2$\theta$ min. (°) | 5.66 |
| Measured reflections | 1059 |
| $R_{int}$ | 0.0667 |
| Unique reflections | 923 |
| Observed reflection [$\|F\| > 4\sigma(F)$] | 689 |
| *F* (000) | 624 |
| *Refinement* | |
| Final *R* (%)/*wR*2 (%) | 9.59/25.59 |
| Goodness-of-fit on $F^2$ (*S*) | 0.965 |
| $\Delta\rho_{max}$ (e.Å$^{-3}$)/$\Delta\rho_{min}$(e.Å$^{-3}$) | 0.421/−0.509 |
| No. of restraints/parameters | 57/175 |
| Data[$\|F\| > 4\sigma(F)$]-to-parameter ratio | 3.57:1 |

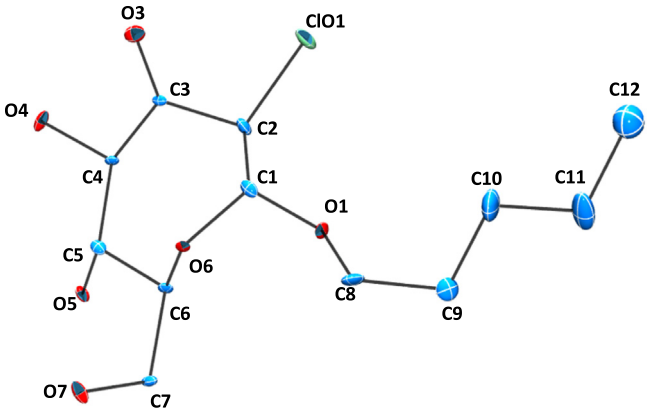


**Figure 1.** ORTEP of **1**, with displacement ellipsoids, at a 10% probability level.

**Table 2**
Selected bond lengths (estimated standard deviations in parentheses)

| Bond | Length (Å) | Bond | Length (Å) |
|---|---|---|---|
| O6—C1 | 1.41 (0.01) | C5—H5A | 0.98 |
| C1—C2 | 1.60 (0.03) | C5—O5 | 1.41 (0.02) |
| C2—C3 | 1.51 (0.02) | O5—H5 | 0.82 |
| C3—C4 | 1.55 (0.02) | C6—H6 | 0.98 |
| C4—C5 | 1.50 (0.02) | O1—C8 | 1.43 (0.02) |
| C5—C6 | 1.50 (0.02) | C8—H8A | 0.97 |
| C6—O6 | 1.47 (0.02) | C8—H8B | 0.97 |
| C6—C7 | 1.56 (0.02) | C8—C9 | 1.54 (0.02) |
| C1—O1 | 1.40 (0.02) | C9—H9B | 0.97 |
| C1—H1 | 0.98 | C9—H9A | 0.97 |
| C2—Cl | 1.78 (0.01) | C9—C10 | 1.46 (0.03) |
| C2—H2 | 0.98 | C10—H10A | 0.97 |
| C3—O3 | 1.19 (0.02) | C10—H10B | 0.97 |
| C4—H4A | 0.98 | C10—C11 | 1.53 (0.02) |
| C4—O4 | 1.44 (0.02) | C11—H11A | 0.97 |
| O4—H4 | 0.82 | C11—H11B | 0.98 |
| C12—H12A | 0.96 | C11—C12 | 1.54 (0.02) |
| C12—H12B | 0.96 | | |
| C12—H12C | 0.96 | | |

**Table 3**
Selected bond angles (estimated standard deviations in parentheses)

| Bonds | Angle (°) | Bonds | Angle (°) |
|---|---|---|---|
| O6—C1—C2 | 112.6 (0.9) | H8A—C8—H8B | 108.0 |
| C1—C2—C3 | 108.2 (1.3) | H9B—C9—H9A | 107.8 |
| C3—C4—C5 | 121.5 (1.2) | C9—C10—H10A | 108.7 |
| C5—C6—O6 | 109.9 (1.1) | C9—C10—H10B | 108.7 |
| O1—C1—O6 | 112.7 (1.3) | C10—C11—H11A | 108.7 |
| O1—C1—C2 | 101.2 (1.3) | C10—C11—H11B | 108.7 |
| C1—C2—Cl | 105.9 (0.9) | H10B—C10—C11 | 108.7 |
| Cl—C2—C3 | 111.5 (1.1) | H10A—C10—C11 | 108.7 |
| C2—C3—O3 | 122.6 (1.1) | H11B—C11—C12 | 108.7 |
| O3—C3—C4 | 122.5 (1.1) | H11A—C11—C12 | 108.7 |
| C3—C4—O4 | 108.3 (1.2) | H12A—C12—C11 | 109.5 |
| O4—C4—C5 | 111.1 (1.1) | H12B—C12—C11 | 109.5 |
| C4—C5—O5 | 110.7 (1.4) | H12C—C12—C11 | 109.5 |
| C4—C5—C6 | 114.4 (1.1) | H12C—C12—H12A | 109.5 |
| C2—C3—C4 | 114.7 (1.2) | H12C—C12—H12B | 109.5 |
| C5—C6—C7 | 114.0 (1.1) | H12A—C12—H12B | 109.5 |
| C6—C7—O7 | 113.9 (1.2) | H12C—C12—C11 | 109.5 |
| C8—O1—C1 | 112.3 (1.6) | C4—O4—H4 | 109.5 |
| O1—C8—C9 | 111.3 (1.9) | C3—C4—H4A | 104.9 |
| C10—C9—C8 | 112.6 (1.8) | C4—C5—HA | 108.2 |
| C11—C10—C9 | 114.2 (2.1) | O4—C4—H4A | 104.9 |
| C7—C6—O6 | 101.5 (1.3) | C8—C9—H9A | 109.1 |
| C1—O6—C6 | 115.5 (1.1) | C8—C9—H9B | 109.1 |
| O5—C5—C6 | 107.1 (1.2) | C1—C2—H2 | 110.4 |
| O1—C1—C2 | 101.2 (1.3) | Cl—C2—H2 | 110.4 |
| C6—C7—H7A | 108.8 | C5—C6—H6 | 110.4 |
| C6—C7—H7B | 108.8 | H6—C6—C7 | 110.4 |
| C5—O5—H5 | 109.5 | | |

66.1°, indicating a *gauche* conformation. The torsion angle of O1—C1—C2—ClO1 of −80.3° and O6—C1—C2—ClO1 of 159.1° indicated that the chlorine substituent resided in *gauche–trans* orientation with respect to the septanoside ring (Table 4).

A contiguous positive sign and remaining alternate positive and negative signs of dihedral angles represented a twist-chair conformation.[16] The torsional angles observed for septanoside derivative **1** were matched with the computed torsional angles of oxepanes (Table 5). The observed torsional angles are very close to twist-chair torsional angles of oxepane, reported by Strauss and co-workers.[16]

In the present case, the C6—O6—C1—C2 and O6—C1—C2—C3 torsion angles were 48.7° and 39.6°, respectively, leading to select the least-square plane passing through O6, C1, and C2. The calculation showed that the plane consisted of O6, C1, and C2 passing through close to the midpoint of C4—C5 bond. This observation pointed that the septanoside ring adopted a deviated twist-chair conformation and represented as $^{5,6}TC_{3,4}$.

**Table 4**
Selected torsion angles (estimated standard deviations in parentheses)

| Septanoside ring | Angle (°) |
|---|---|
| O5—C5—C4—O4 | 73.9 (1.5) |
| O6—C1—C2—C3 | 39.6 (1.7) |
| C1—C2—C3—C4 | −85.9 (1.5) |
| C2—C3—C4—C5 | 60.8 (1.9) |
| C3—C4—C5—C6 | −36.1 (1.9) |
| C4—C5—C6—C7 | 176.5 (1.4) |
| C4—C5—C6—O6 | 63.3 (1.6) |
| C5—C6—O6—C1 | −102.2 (1.3) |
| C5—C6—C7—O7 | −53.3 (1.7) |
| O1—C1—O6—C6 | −65.0 (1.6) |
| O1—C1—C2—Cl | −80.3 (1.2) |
| O1—C1—C2—C3 | 160.1 (1.1) |
| Cl—C2—C3—O3 | −16.3 (2.2) |
| C1—C2—C3—O3 | 99.7 (1.8) |
| C2—C3—C4—O4 | −169.0 (1.4) |
| O3—C3—C4—O4 | 5.5 (2.0) |
| O3—C3—C4—C5 | −124.8 (1.6) |
| C3—C4—C5—O5 | −157.1 (1.1) |
| O5—C5—C6—C7 | −60.6 (1.6) |
| C4—C3—C2—ClO1 | 158.1 (1.1) |
| C6—O6—C1—C2 | 48.7 (1.6) |
| O4—C4—C5—C6 | −165.1 (1.2) |
| O1—C6—C7—O7 | 64.8 (1.3) |
| O6—C6—C5—O5 | −173.8 (1.2) |
| ClO1—C2—C1—O6 | 159.1 (1.0) |
| C7—C6—O6—C1 | 136.8 (1.1) |
| C8—O1—C1—C2 | 166.3 (1.2) |
| C8—O1—C1—O1 | −73.2 (1.5) |
| C1—O1—C8—C9 | −153.6 (1.4) |
| C8—C9—C10—C11 | −175.9 (2.2) |
| C9—C10—C11—C12 | 176.2 (2.5) |
| O1—C8—C9—C10 | 66.1 (2.5) |

**Table 5**
Torsional angles of **1**, compared with the values computed for the twist-chair conformation of oxepane

| Sequence | **1** | Computed torsional angles | |
|---|---|---|---|
| | | Twist-boat | Twist-chair |
| O6—C1—C2—C3 | 39.6 | −46.6 | 44.4 |
| C1—C2—C3—C4 | −85.9 | −34.2 | −90.9 |
| C2—C3—C4—C5 | 60.8 | 83.7 | 67.7 |
| C3—C4—C5—C6 | −36.1 | −70.0 | −50.8 |
| C4—C5—C6—O6 | 63.3 | 54.3 | 72.9 |
| C5—C6—O6—C1 | −102.2 | −80.2 | −96.4 |
| C6—O6—C1—C2 | 48.7 | 101.9 | 43.0 |

Atoms C3 and C4 are displaced 0.92 Å and 0.26 Å, respectively, on one side, whereas C5 and C6 are displaced 0.33 Å and 0.99 Å, respectively, on the other side of the least-square plane. The anomeric substituent displaced 1.28 Å from the mean plane, while chlorine at C2 is 0.61 Å away from the plane (Fig. 2).

The torsional angle C4—C3—C2—C1 was −85.9°, which forced Cl01—C2—C1—O6 torsional angle to be 159.3°, so as to avoid the *endo*-cyclic oxygen and chloride lone pair-lone pair electron repulsion. The constrained torsional angle O4—C4—C3—O3 of 5.5° indicated an eclipsing interaction between O3 and O4—H4, which in turn, facilitated intermolecular hydrogen bonding interactions (vide infra).

An analysis of the non-covalent interactions showed that an array of inter- and intramolecular hydrogen bonding interactions stabilized the molecular packing in **1**. The hydrogen bonding interactions were identified by the inter-atomic distances between oxygen atoms and the hydrogen atoms of the hydroxyl groups. The

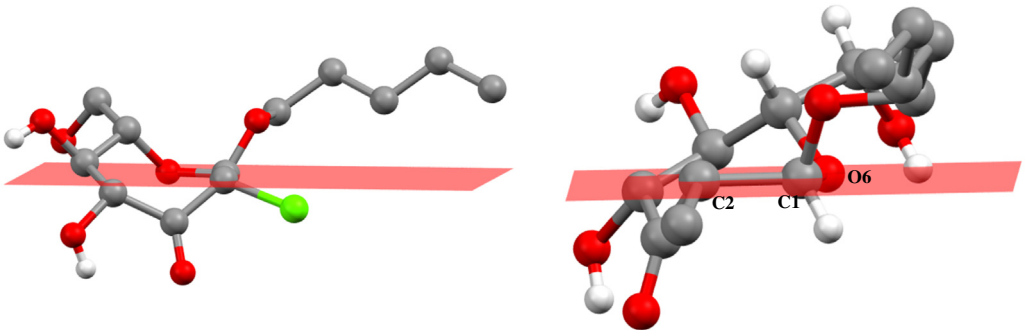


**Figure 2.** Structure of **1**, with mean plane passing through O6, C1, and C2. Left: plane back view; right: plane front view.

**Table 6**
The hydrogen bond distance and angles, with symmetry code

| Donor | Acceptor | D···A (Å) | H···A (Å) | D—H···A (°) |
|---|---|---|---|---|
| *Intramolecular hydrogen bond* | | | | |
| O4 | O3 | 2.65 | 2.21 | 113.9 |
| *Intermolecular hydrogen bond* | | | | |
| O4 | O5 ($x, y-1, z$) | 2.95 | 2.40 | 125.5 |
| O5 | O7 ($-x+1, y, -z$) | 2.71 | 2.07 | 133.9 |
| O7 | O4 ($x, y. z-1$) | 2.80 | 2.15 | 136.2 |

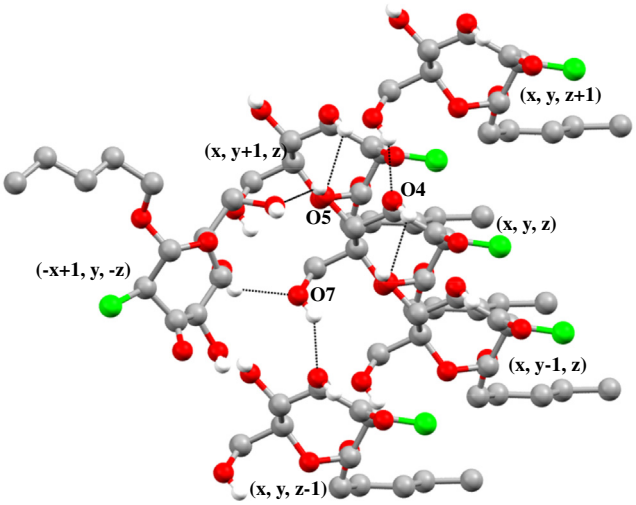


**Figure 3.** Intermolecular hydrogen bonding interactions in **1**.

O—H···O bonds were identified based on the distance criterion of H···O <3.0 Å and the angle of O—H···O >90°.[1] The hydrogen bond distances and the angles for **1** are given in Table 6. The hydrogen bond O5—H5···O4 was the shortest (2.07 Å), whereas O4—H4···O5 was found to be longest (2.40 Å). The hydroxyl groups O4—H4, O5—H5, and O7—H7 acted both as hydrogen bond donors and as acceptors.

Each molecule interacted with neighbors, through six intermolecular hydrogen bonding interactions (Fig. 3). Two intermolecular hydrogen bonds formed between the pairs related by two-fold rotation along crystallographic '*b*' axis and rest of the four formed between the unit translated molecules along '*b*' and '*c*' axes. A three-centered hydrogen bond formed between O3, O5, and H4 (O4), where O4—H4 was a bifurcated donor for an intramolecular hydrogen bond in O4—H4···O3 and an intermolecular hydrogen bond in O4—H4···O5 ($x, y-1, z$). The overall O—H···O hydrogen bonding interactions are shown in Figures 4 and 5.

Apart from hydrogen-bonding interactions, C—H···O bonding[17] was also observed. It is characterized by the acidity of the C—H bond and also the nature of basicity of the O-atom, or acceptor atom.[18,19] The C—H···O bonds were identified based on the distance criterion of <2.8 Å (H···O) and the angle of C—H···O >120°.[20] The carbonyl O-atom could participate in as many as four C—H···O interactions, on the basis of this criterion. The carbonyl oxygen at C3 participated in four C—H···O interactions, namely, C4—H4A, C2—H2, C8—H8B, and C6—H6. Such multiple C—H···O interactions are known previously.[20] The bond angles and the distances for C—H···O interactions were within the cut-off value, as given in Table 7. Among the several interactions, C2—H2···O was stronger than remaining C—H···O interactions. The C—H···O interactions within the radius of 4 Å of the carbonyl oxygen (O3) are shown in Figure 6.

Molecular packing shows that there exists a bi-layer arrangement of the molecules, with sugar head–head interactions phase

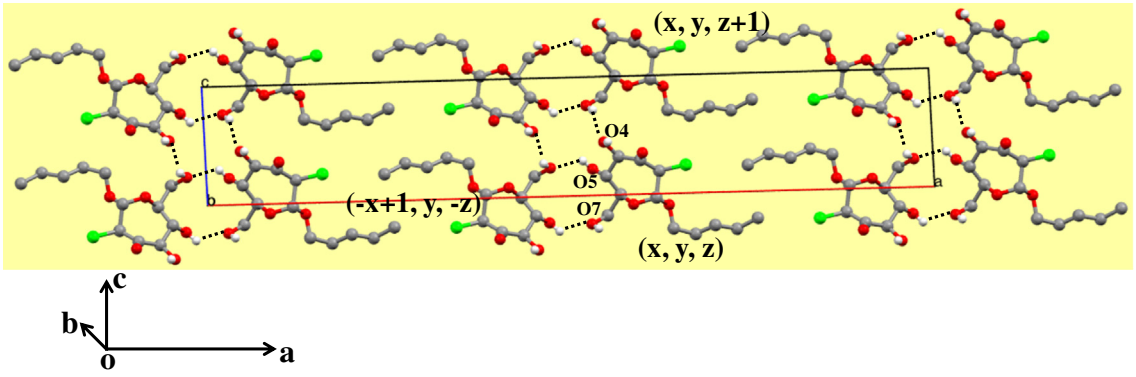


**Figure 4.** Molecular packing and O—H···O interactions along crystallographic '*b*' axis.

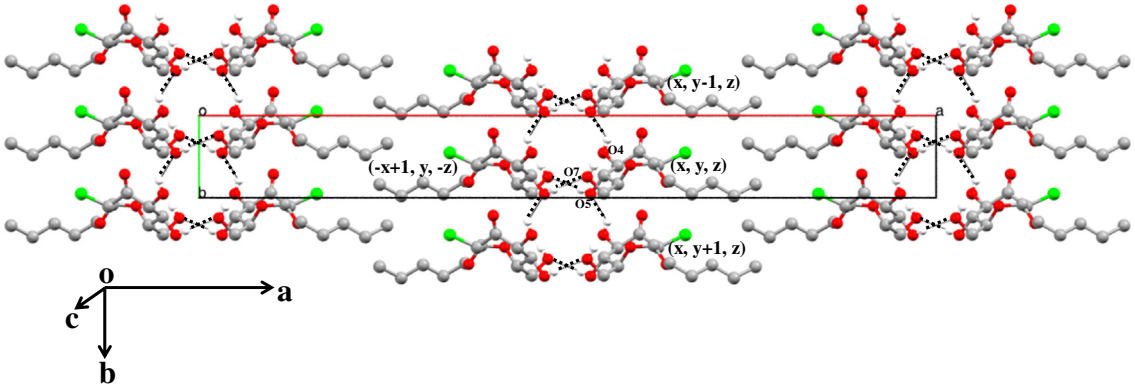


**Figure 5.** Molecular packing and O—H···O interactions along crystallographic '*c*' axis.

**Table 7**
Hydrogen bond parameters of C—H···O interactions

| Donor | Acceptor | D···A (Å) | H···A (Å) | D—H···A (°) |
|---|---|---|---|---|
| C2 ($x, y-1, z$) | O3 ($x, y, z$) | 3.28 | 2.36 | 156.2 |
| C4 ($x, y-1, z$) | O3 ($x, y, z$) | 3.25 | 2.45 | 138.2 |
| C6 ($x, y-1, z$) | O3 ($x, y, z$) | 3.34 | 2.52 | 141.1 |
| C8 ($x, y-1, z+1$) | O3 ($x, y, z$) | 3.57 | 2.72 | 146.2 |

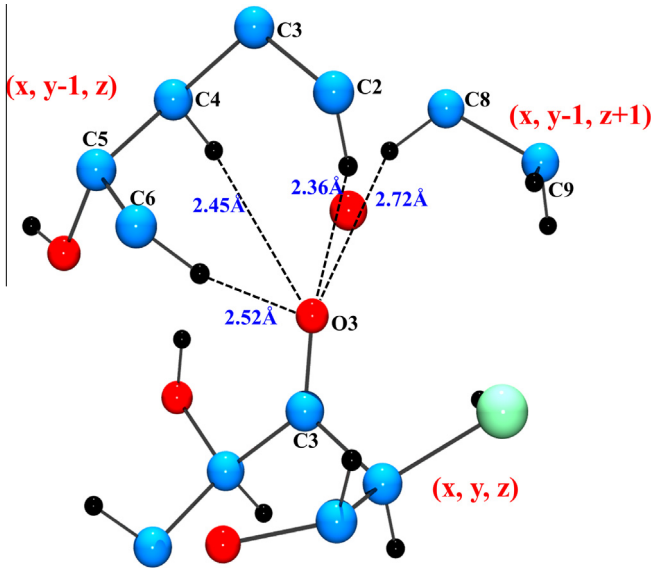


**Figure 6.** Environment of the atom O3 within the radius of 4 Å, showing the C—H···O interactions.

segregate from the lypophilic alkyl chains. Whereas, head group involved O—H···O and C—H···O interactions, van der Waals interaction across alkyl chains was seen, within a distance 2.40 Å between adjacent layers. The van der Waals interaction induced interdigitization of the terminal methyl group of alkyl chain was seen, whereas the chloride substituent resided in the hydrophobic region of the bilayer structure. Dense, infinite hydrogen-bonding and other non-covalent interactions within and across the planar bilayer result in a highly-ordered molecular packing in the crystal lattice.

## 3. Conclusion

Single crystal X-ray structural determination and analysis of **1** show a conformation $^{5,6}TC_{3,4}$, which differs uniquely from all known crystal structures of septanoside derivatives. An important outcome of the structural analysis is in realizing a dense network of non-covalent interactions. These interactions are O—H···O and C—H···O interactions, in which carbonyl oxygen maximizes the C—H···O interactions. On the other hand, participation of hydroxyl group and carbonyl oxygen in intra- and intermolecular hydrogen bonding interactions, C—H···O and van der Waals interactions stabilize the highly-ordered arrangement of the molecules in the crystal lattice.

## 4. Experimental

### 4.1. *n*-Pentyl-2-chloro-2-deoxy-α-D-*manno*-sept-3-uloside (1)

A solution of chloro-oxepine **2**[15b] (0.050 g, 0.076 mmol) in MeOH (10 mL) was added with Pd/C (10%, 0.04 g) and the mixture was stirred under a positive pressure of $H_2$ gas for 12 h. The reaction mixture was filtered over a celite pad and washed with MeOH (3 × 10 mL), and solvent removed in vacuo. The resulting residue was purified ($CHCl_3$/MeOH = 4:1), to afford *n*-pentyl-2-chloro-2-deoxy-α-D-*manno*-sept-3-uloside **1** (0.020 g, 93%) as colorless crystalline solid, mp 139–141 °C. $[\alpha]_D$ −5.04 (*c* 0.5, MeOH); $^1$H NMR (400 MHz, $CD_3OD$) $\delta$ 5.00 (d, $J$ = 7.4 Hz, 1H), 4.66 (d, $J$ = 7.6 Hz, 1H), 4.34 (d, $J$ = 7.6 Hz, 1H), 4.11–4.06 (m, 1H), 3.92 (dt, $J$ = 13.2, 3.2 Hz, 1H), 3.82 (dd, $J$ = 12.0, 2.4 Hz, 1H), 3.71 (dd, $J$ = 12.0, 4.8 Hz, 1H), 3.51 (dt, $J$ = 9.2, 6.4 Hz, 1H), 3.40 (dd, $J$ = 10.2, 6.4 Hz, 1H), 1.63–1.58 (m, 2H), 1.40–1.34 (m, 4H), 0.92 (t, $J$ = 6.8 Hz, 3H); $^{13}$C NMR (100 MHz, $CD_3OD$) $\delta$ 200.6, 103.1, 83.8, 74.3, 72.0, 70.0, 63.2, 62.9, 30.0, 29.3, 23.4, 14.3; ESI-MS: *m*/*z* $C_{12}H_{21}O_6ClNa$ calcd for 319.0924; found: 319.0928.

### 4.2. Crystal structure analysis

Single crystals of **1** suitable for X-ray diffraction analysis, were grown by slow evaporation from MeOH. X-ray diffraction datasets were collected using Mo$K_\alpha$ (0.71073 Å) radiation, on a BRUKER AXS KAPPA APEXII CCD diffractometer. Data collection was carried out in $\phi$ and $\omega$ scan type mode using the crystals at 296 K. The structure was solved by direct methods using SHELXD.[21] Large $E$ values ($E$ >1.2) were employed to obtain the structure solution from random phases, followed by peak list optimization. The final correlation coefficient[22] was 83.31%, suggesting a good initial model for refinement. Refinement for the structure was carried out against $F^2$ with full matrix least-squares method using SHELXL-97.[23] All the non-hydrogen atoms were initially refined isotropically. All the hydrogen atoms were fixed geometrically in idealized positions and allowed to ride with the C or O atoms to which they were bonded, in the final cycles of refinement. The final *R*-factor

obtained was 0.0959 ($wR_2 = 0.2559$) for 689 observed reflections with $|Fo| > 4\sigma(F)$. The function minimized during the refinement was $\sum w(|Fo| - |F|)^2$, $w = 1/[\sigma^2 \times (Fo^2) + (0.1516 \times P)^2 + 13.1192 \times P]$, where $P = (\max(Fo^2, 0) + 2Fc^2)/3$.

## Acknowledgements

We thank the Department of Science and Technology, New Delhi, for a financial support. S.D. thanks Council of Scientific and Industrial Research, New Delhi, for a senior research fellowship.

## Supplementary data

The crystallographic data was deposited at the Cambridge Structural database (Accession number CCDC 991870). Copies of this can be obtained free of charge from the Director, CCDC, 12 Union Road, Cambridge, UK (fax: +44 1223 336033; e-mail: deposit @ccdc.cam.ac.uk or http://www.ccdc.cam.ac.uk).

Supplementary data associated with this article can be found, in the online version, at http://dx.doi.org/10.1016/j.carres.2014.04.019.

## References

1. (a) Jeffrey, G. A.; Saenger, W. *Hydrogen Bonding in Biological Structures*; Springer Verlag: Berlin, 1991; (b) Masuda, M.; Shimizu, T. *Carbohydr. Res.* **2000**, *326*, 55–66.
2. (a) Pakulski, Z. *Pol. J. Chem.* **2006**, *80*, 1293–1326; (b) Saha, J.; Peczuh, M. W. *Adv. Carbohydr. Chem. Biochem.* **2011**, *66*, 121–186.
3. Jackobs, J.; Sundaralingam, M. *J. Chem. Soc., Chem. Commun.* **1970**, 157–159.
4. Jackobs, J.; Reno, M. A.; Sundaralingam, M. *Carbohydr. Res.* **1973**, *28*, 75–85.
5. James, V. J.; Stevens, J. D. *Carbohydr. Res.* **1980**, *82*, 167–174.
6. Wood, R. A.; James, V. J.; Rae, A. D.; Stevens, J. D.; Moore, F. H. *Aust. J. Chem.* **1983**, *36*, 2269–2277.
7. Pallister, E. T.; Stephenson, N. C.; Stevens, J. D. *J. Chem. Soc., Chem. Commun.* **1972**, 98–99.
8. McConnell, J. F.; Stevens, J. D. *J. Chem. Soc., Perkin Trans. 2* **1974**, 77–81.
9. Beale, J. P.; Stephenson, N. C.; Stevens, J. D. *J. Chem. Soc., Chem. Commun.* **1971**, 484–486.
10. Craig, D. C.; James, V. J.; Stevens, J. D. *Aust. J. Chem.* **1990**, *43*, 2083–2086.
11. Bhadbhade, M.; Craig, D. C.; Ng, C. J.; Odier, L.; Stevens, J. D. *Carbohydr. Res.* **2012**, *353*, 86–91.
12. Peczuh, M. W.; Snyder, N. L.; Fyvie, W. S. *Carbohydr. Res.* **2004**, *339*, 1163–1171.
13. Jackowski, O.; Chrétien, F.; Didierjean, C.; Chapleur, Y. *Carbohydr. Res.* **2012**, *365*, 93–103.
14. (a) Ganesh, N. V.; Jayaraman, N. *J. Org. Chem.* **2007**, *72*, 5500–5504; (b) Ganesh, N. V.; Jayaraman, N. *J. Org. Chem.* **2009**, *74*, 739–746; (c) Ganesh, N. V.; Raghothama, S.; Sonti, R.; Jayaraman, N. *J. Org. Chem.* **2010**, *75*, 215–218.
15. (a) Dey, S.; Jayaraman, N. *Beilstein J. Org. Chem.* **2012**, *8*, 522–527; (b) Dey, S.; Jayaraman, N. *Carbohydr. Res.* **2014**, *319*, 66–71.
16. Bocian, D. F.; Strauss, H. L. *J. Am. Chem. Soc.* **1977**, *99*, 2876–2882.
17. (a) Sutor, D. J. *Nature* **1962**, *195*, 68–69; (b) Sutor, D. J. *J. Chem. Soc.* **1963**, 1105–1110.
18. Desiraju, G. R. *J. Chem. Soc., Chem. Commun.* **1989**, 179–180.
19. Steiner, T. *J. Chem. Soc., Chem. Commun.* **1994**, 2341–2342.
20. Desiraju, G. R. *Acc. Chem. Res.* **1996**, *29*, 441–449.
21. Schneider, T. R.; Sheldrick, G. M. *Acta Crystallogr., Sect. D* **2002**, *58*, 1772–1779.
22. Fujinaga, M.; Read, R. J. *J. Appl. Crystallogr.* **1987**, *20*, 517–521.
23. (a) Sheldrick, G. M. *SHELXL-97, A Program for Crystal Structure Refinement*; University of Göttingen: Göttingen, 1997; (b) Sheldrick, G. M. *Acta Crystallogr., Sect. A* **2008**, *64*, 112–122.